Neuroendocrine tumors of the lung: major radiologic findings in a series of 22 histopathologically confirmed cases*

Tumores neuroendócrinos do pulmão: principais achados radiológicos em uma série de 22 casos com confirmação anatomopatológica

Marcel Koenigkam Santos[1], André Rodrigues Façanha Barreto[2], Francisco Abaeté Chagas Neto[3], Valdair Francisco Muglia[4], Jorge Elias Júnior[5]

Abstract

Objective: To describe key imaging findings in a series of cases of primary neuroendocrine tumors of the lung (NTLs), with emphasis on computed tomography changes. **Materials and Methods:** Imaging studies of 22 patients (12 men, mean age 60 years) with histopathologically confirmed diagnosis, evaluated in the authors's institution during the last five years were retrospectively reviewed by two radiologists, with findings being consensually described focusing on changes observed at computed tomography. **Results:** The authors have described five typical carcinoids, three atypical carcinoids, three large-cell neuroendocrine carcinomas (LCNCs), and 11 small-cell lung cancers (SCLCs). Only one typical carcinoid presented the characteristic appearance of central endobronchial nodule with distal pulmonary atelectasis, while the others were pulmonary nodules or masses. The atypical carcinoids corresponded to peripheral heterogeneous masses. One out of the three LCNCs was a peripheral homogeneous mass, while the others were ill-defined and heterogeneous. The 11 SCLCs corresponded to central, infiltrating and heterogeneous masses with secondary pleuropulmonary changes. Calcifications were absent both in LGNCs and SCLCs. Metastases were found initially and also at follow-up of all the cases of LCNCs and SCLCs. **Conclusion:** Although some imaging features may be similar, radiologic findings considered together with clinical information may play a relevant role in the differentiation of histological types of NTLs.
Keywords: Computed tomography; Lung neoplasms; Neuroendocrine tumors.

Resumo

Objetivo: Descrever os principais achados de imagem em uma série de casos de tumores neuroendócrinos primários do pulmão (TNPs), destacando as alterações na tomografia computadorizada. **Materiais e Métodos:** Exames de 22 pacientes (12 homens, idade média de 60 anos) avaliados nos últimos cinco anos em nosso serviço, com confirmação histopatológica, foram retrospectivamente revistos por dois médicos radiologistas e os achados foram descritos em consenso, focando as alterações tomográficas. **Resultados:** Descrevemos 5 carcinoides típicos, 3 carcinoides atípicos, 3 carcinomas neuroendócrinos de grandes células (CNGCs) e 11 cânceres pulmonares de pequenas células (CPPCs). Apenas um carcinoide típico apresentou aspecto característico de nódulo endobrônquico central com atelectasia pulmonar distal, enquanto os demais foram nódulos ou massas pulmonares. Os carcinoides atípicos eram massas pulmonares periféricas e heterogêneas. Um CNGC era massa periférica delimitada e homogênea, enquanto os demais eram mal delimitados e heterogêneos. Os 11 CPPCs eram massas centrais, infiltrativas e heterogêneas, com alterações pleuropulmonares secundárias. Calcificações estavam ausentes nos CNGCs e CPPCs. Metástases foram vistas inicialmente ou no seguimento de todos os CNGCs e CPPCs. **Conclusão:** Apesar de alguns aspectos semelhantes nos exames de imagem, os achados radiológicos, quando integrados às informações clínicas, podem constituir critérios importantes na diferenciação dos tipos histológicos de TNPs.
Unitermos: Tomografia computadorizada; Neoplasias pulmonares; Tumores neuroendócrinos.

INTRODUCTION

In clinical routine, primary lung tumors originated in the airways or in the alveoli are usually divided into small-cell lung cancer (SCLC) and non-small cell lung cancer (NSCLC), the first one being the

most aggressive type, with worse prognosis, and clinical staging and therapeutic approach different from the other tumor types. Among the different types of NSCLC, most commonly described are the adenocarcinoma and squamous-cell carcinoma, the former currently being the most frequently found in most studied populations[1]. Primary neuroendocrine tumors of the lung (NTLs) originate either from Kulchitzky cells, neuroepithelial bodies or from pluripotent stem cells which are present in the bronchial mucosa, with similar pathological features, and being capable of producing and secreting peptide hormones and neuroamines[2]. Since the early 1990's, because of its clinical and histological characteristics, SCLC is classified as a neuroendocrine neoplasia of the lung. Neuroendocrine tumors of the lung comprise 25% of all lung neoplasms, with a wide spectrum of clinical behaviors, being currently classified into four types: typical carcinoid tumor (low malignancy grade), atypical carcinoid tumor (intermediate malignancy grade), large-cell neuroendocrine carcinomas (LCNC) and SCLC, these both with high malignancy grade, the latter representing most of the primary neuroendocrine lung lesions[3,4].

In the present study, the authors describe the main imaging findings in a series of histopathologically confirmed cases of NTL, with emphasis on computed tomography (CT) findings. Also, the authors make a brief description of the main clinical data, including information on the evolution of the cases, correlating them with radiological and anatomopathological data.

MATERIALS AND METHODS

Clinical data and imaging studies of patients diagnosed with NTL in the authors' institution over the previous five years were retrospectively reviewed. Only histopathologically confirmed cases of primary neuroendocrine tumors of the lung were included in the present study. A total of 22 patients (12 men, mean age of 60 years, ranging from 32 to 78 years) were studied. Considering the retrospective nature of the study, with exams that are part of the clinical routine in the assessment of such patients, it exempted a term of free and informed consent in addition to the one obtained previously to the performance of the exams. Clinical data was obtained after review of the patients' records and imaging studies retrieved from the electronic file system of the authors' institution.

Images were reviewed by two radiologists, and the findings were described in consensus. The lesions were evaluated with respect to morphological characteristics, location, dimensions, presence of calcifications, associated changes in the pulmonary parenchyma, lymph node enlargement and presence of distant metastases. All the imaging studies stored in the electronic file system were reviewed, including plain radiographs and magnetic resonance imaging (MRI) studies, but the reviewers have particularly focused on the description of CT findings, which is currently the most accurate radiological method and most commonly utilized in the evaluation of lung tumors. In spite of not being related to the main objective of the present study, the post-treatment follow-up exams, whenever available, were also reviewed for correlation of imaging findings with the clinical progression according to the type of neoplasia identified at the anatomopathological study.

RESULTS

Current or previous smoking habit was reported by all the patients, independently of the histological tumor type. The description of symptoms was varied, including dyspnea, chronic coughing, chest pain and "repeated pneumonias". Systemic symptoms, such as weight loss and malaise, were decribed with higher frequency in cases of LCNC and SCLC. Along the medical records review process, data confirming the presence of paraneoplastic syndrome due to ectopic production of hormones were not found for any of the patients. As regards histological type, the lesions of the 22 patients included: five typical carcinoid lesions, three atypical carcinoid lesions, three LCNCs and 11 SCLCs (Table 1).

Among the five patients with typical carcinoid lesions, only one (20%) had a well defined central endobronchial nodule with soft tissue density in association with distal lung atelectasis[5] (Figure 1). Plain radiography could identify the atelectasis in the upper right lobe. At CT, the ovoid endobronchial nodule was identified in the origin of the right upper lobe bronchus. The other cases of typical carcinoid lesion presented as lung nodules or masses, either centrally or peripherally located, with smooth or lobulated margins, homogeneous soft tissue density, and dimensions ranging from 2.1 to 5.5 cm in the largest diameter (Figures 2 and 3). Calcifications were found in two lesions (40%) and were

Table 1 Summary of clinical and radiological data of the 22 patients diagnosed with primary neuroendocrine tumor of the lung.

	Number of patients	Male	Age in years (variation)	Largest diameter of the lesion (variation)	Chest lymph node enlargement	Metastasis	Clinical progression
Typical carcinoid	5	3 (60%)	32–60	2.1–5.5	0	0	1 (20%) late recurrence after resection
Atypical carcinoid	3	1 (33%)	53–70	3.1–6.0	1 (33%)	2 (67%)	1 (33%) death and 1 progressive disease undergoing treatment
LCNC	3	2 (67%)	36–70	4.2–5.1	2 (67%)	2 (67%)	2 (67%) deaths and 1 progressive disease undergoing treatment
SCLC	11	6 (55%)	46–81	4.9–13.2	11 (100%)	10 (90%)	10 (90%) deaths and 1 undergoing systemic treatment

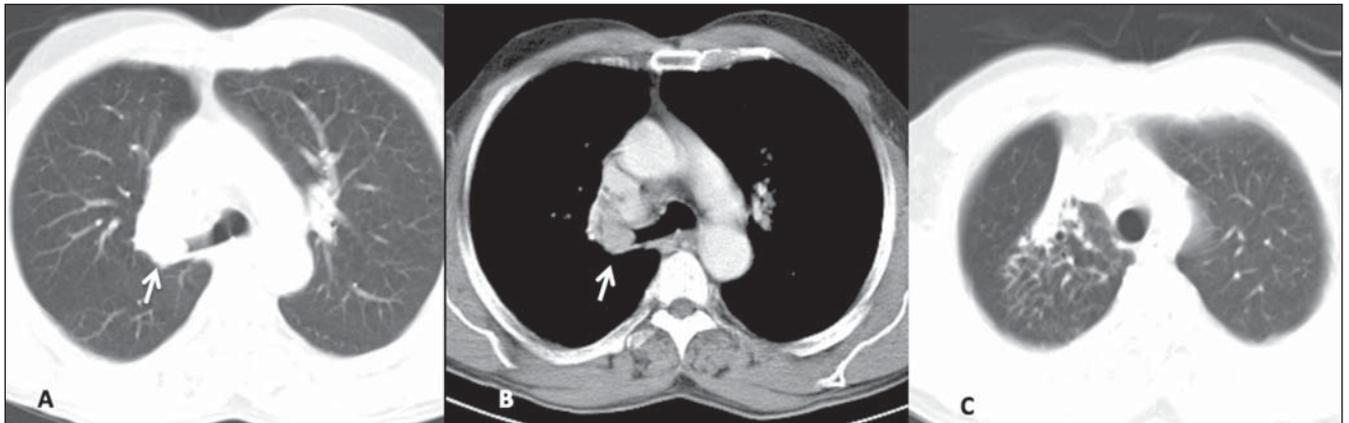LCNC, large-cell neuroendocrine carcinoma; SCLC small-cell lung cancer.

Figure 1. Lesion corresponding to typical carcinoid tumor. Axial chest CT images after intravenous injection of iodinated contrast medium. On the lung window, one may identify the amputation of the upper right lobe bronchus (arrow on **A**) and the distal pulmonary atelectasis (**C**). On the mediastinal window, a well defined, ovoid endobronchial nodule is identified, with homogeneous attenuation (arrow on **B**).
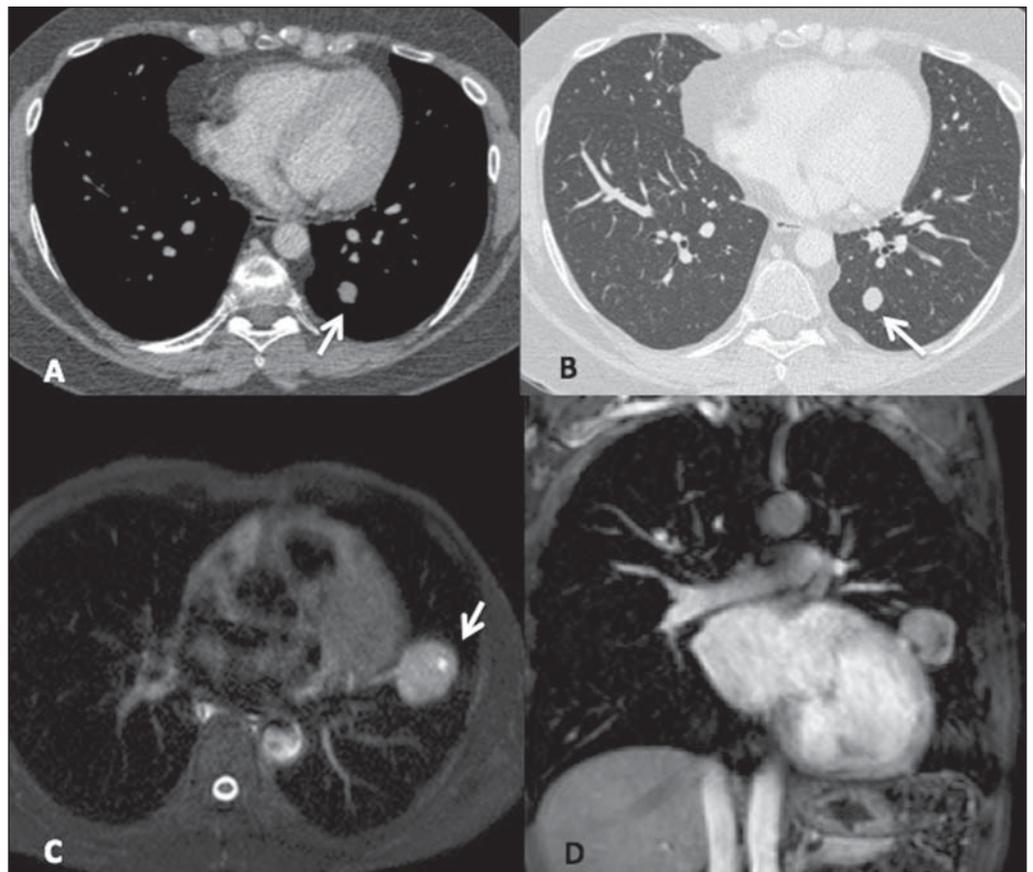

Figure 2. Typical carcinoid tumors. In a 32-year-old patient one has observed an ovoid, homogeneous nodule measuring 1.5 cm in the left lower lobe (arrows), identified at contrast-enhanced, axial chest CT images, on mediastinal (**A**) and lung (**B**) windows. In another patient who underwent MRI, one identifies a well defined mass in the left lung lower lobe, with high signal intensity on T2-weighted sequences (arrow on **C**, axial TSE, T2-weighted image with fat suppression) and a prominent, almost homogeneous contrast enhancement (**D**, coronal GRE T1-weighted image with fat suppression, after administration of paramagnetic contrast medium).

more clearly seen at CT. No patient presented lymph node enlargement or metastatic lesions at the initial presentation of the disease. Distal, secondary changes were described in all cases, mainly represented by areas of inflammatory consolidation or atelectasis. All five patients were submitted to surgical resection (either segmentectomy or lobectomy) and only one patient

presented recurrence of the disease in the clinical follow-up, with mediastinal lymph node enlargement identified six years after diagnosis (Figure 3). One patient with a typical carcinoid lesion also underwent MRI, which demonstrated the presence of a well defined nodule in the left lower lobe with intermediate signal intensity on T1-weighted and hyperintense signal on T2-

weighed sequences, also with restriction in diffusion weighted imaging and prominent contrast-enhancement more noticeable in delayed phases and with homogeneous appearance (Figure 2).

The three cases of atypical carcinoid tumors were identified both at plain radiography and CT, described as peripheral lung masses with lobulated or irregular
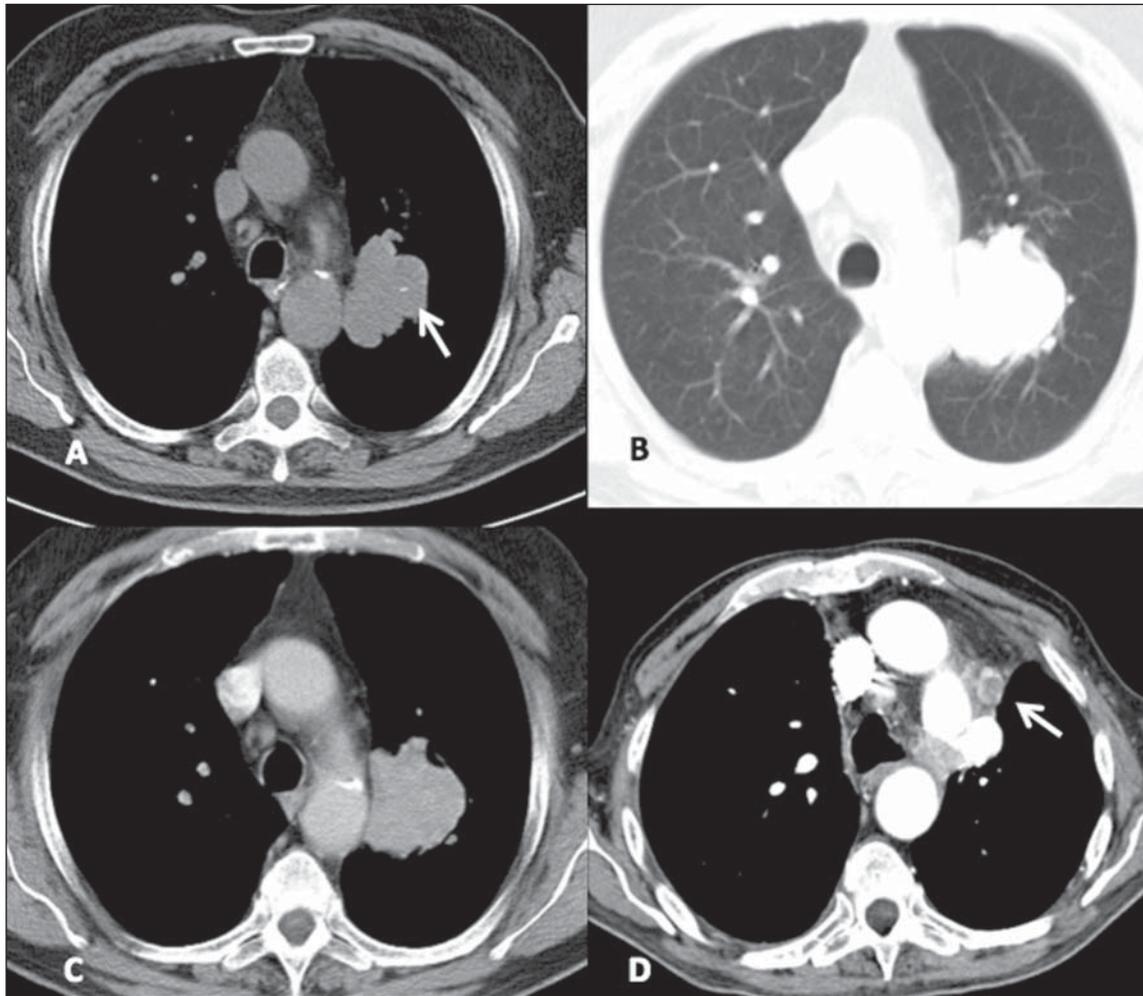
Figure 3. Typical carcinoid tumor. Axial chest CT images show the presence of a lung mass with lobulated contours medially located in the upper left lobe (mediastinal window on **A** and lung window on **B**), with homogeneous density and containing subtle calcifications (arrow on **A**). The post-contrast enhancement is homogeneous (**C**). Late follow-up after resection of the primary lesion shows recurrence of the disease in the form of mediastinal lymphadenopathy (arrow on **D**).

contours, with heterogeneous density and contrast-enhancement, dimensions ranging between 3.1 and 6.0 cm and with secondary changes in the adjacent lung parenchyma (Figure 4). One lesion presented nodular calcifications identified at plain radiography, but best characterized at CT. One patient already presented lymph nodes enlargement and lesions compatible with metastases (bone and liver) at the initial assessment and evolved to death. Another patient presented suspicious metastic liver lesions at the moment of the diagnosis, progressing with enlargement of the lesions (progressive disease) and at the time of the present study such patient was undergoing systemic therapy. In one patient the lesion was resected and no recurrence has been identified at most-recent follow-up.

Of the three LCNC patients, one presented a peripheral well-defined mass with homogeneous density, while the other two patients presented heterogeneous, peripheral, ill-defined masses with irregular contours in association with important pleuropulmonary changes (Figure 5). The lesions dimensions ranged from 4.2 to 5.1 cm and calcifications were not found. The two patients presenting with heterogeneous lesions already presented lymph nodes enlargement and distant metastatic lesions at their initial assessment, and underwent non-surgical therapy, but evolved with progressive disease at follow-up and, later, death. The other patient presented progressive, metastatic disease and currently is still undergoing local and systemic treatment and has not been

submitted to surgical resection of the lung lesion.

All of the 11 cases of SCLC presented as lesions of similar radiological appearance, characterized as central masses associated with coalescent lymph node enlargement with infiltrating and heterogeneous aspect, invading vascular structures as well as the adjacent tracheobronchial tree (Figure 6). Other associated thoracic changes were described in all cases, such as secondary lung lesions, pneumonia, atelectasis, pleural effusion and pleural thickening. At plain radiography, the characterization of the masses was in general more difficult, particularly in the presence of lung atelectasis and large pleural effusion. Distant metastatic lesions were also found in ten patients (90%) at the moment
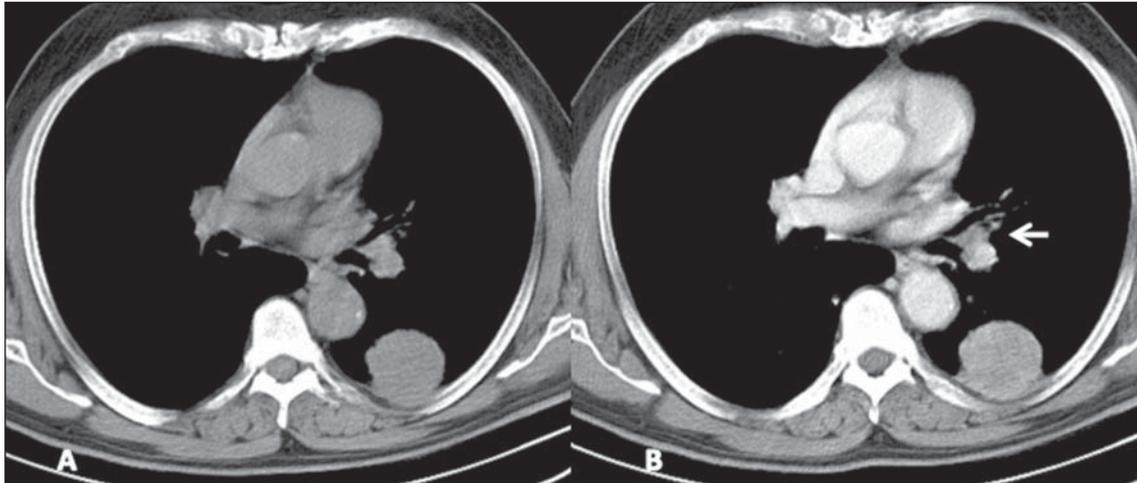
Figure 4. Atypical carcinoid tumor. Pre- (**A**) and post-contrast (**B**) axial chest CT images. Peripheral, well defined mass is identified in the left lower lobe, with almost homogeneous post-contrast enhancement, and in close contact with the pleural surface. Also, notice ipsilateral hilar lymphadenopathy (arrow on **B**).
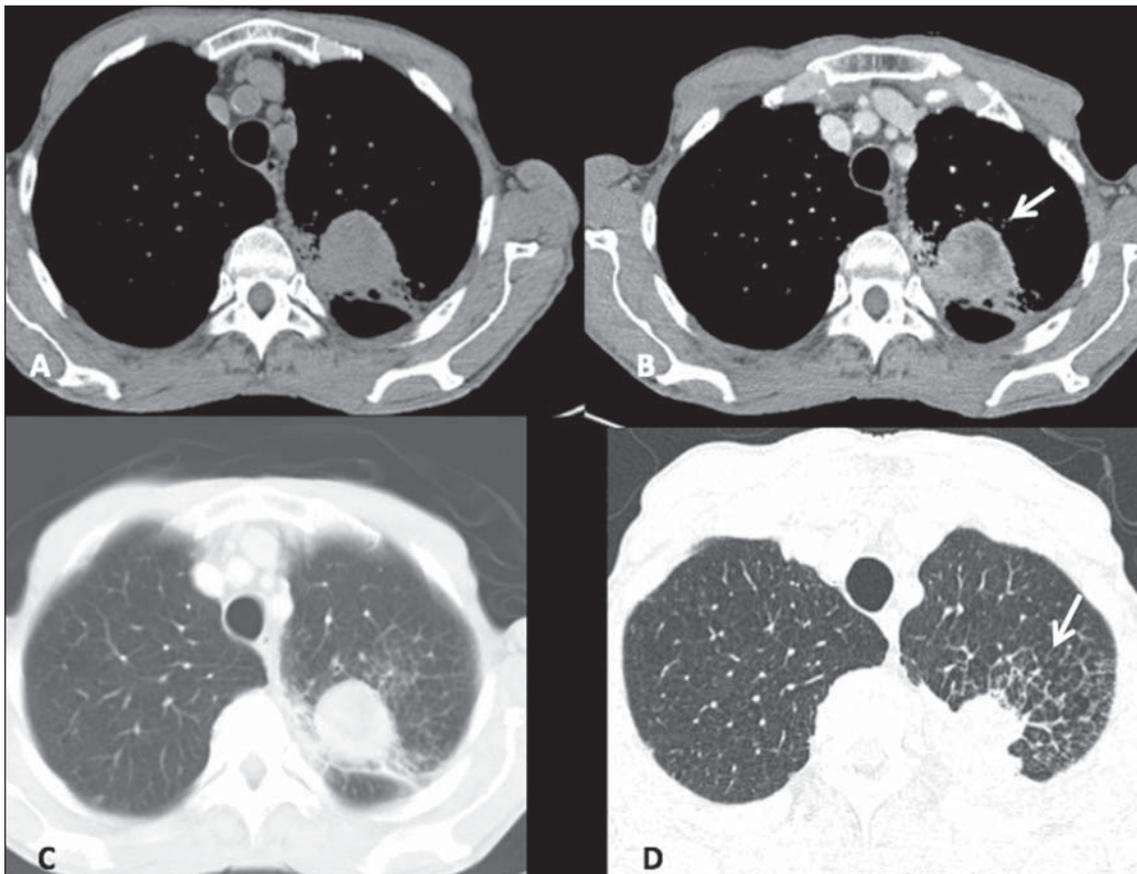

Figure 5. Large-cell neuroendocrine carcinoma. Axial chest CT images, with mediastinal window before (**A**) and after contrast injection (**B**), more images with lung window, with thick slices (**C**) and high resolution, thin sections (**D**). One observes a mass with partially defined limits in the upper left lobe, with heterogeneous post-contrast enhancement (arrow on **B**), in association with secondary changes of the adjacent lung parenchyma, including interstitial thickening due to carcinomatous lymphangitis, best seen on high resolution images (arrow on **D**).

of diagnosis, mainly in bones and upper abdomen (liver and adrenal glands), already seen at the first chest CT scan. In general, the lesions that could be measured were larger than 5.0 cm in their largest diameter, some of them greater than 10.0 cm. Calcifications were not identified in any lesion. Like in the cases of LCNC, all SCLC patients were submitted to local and/or systemic therapy and evolved with progressive disease and death few months after biopsy and histopathological diagnosis, with the exception of one patient who remained under treatment at the moment of the present review.
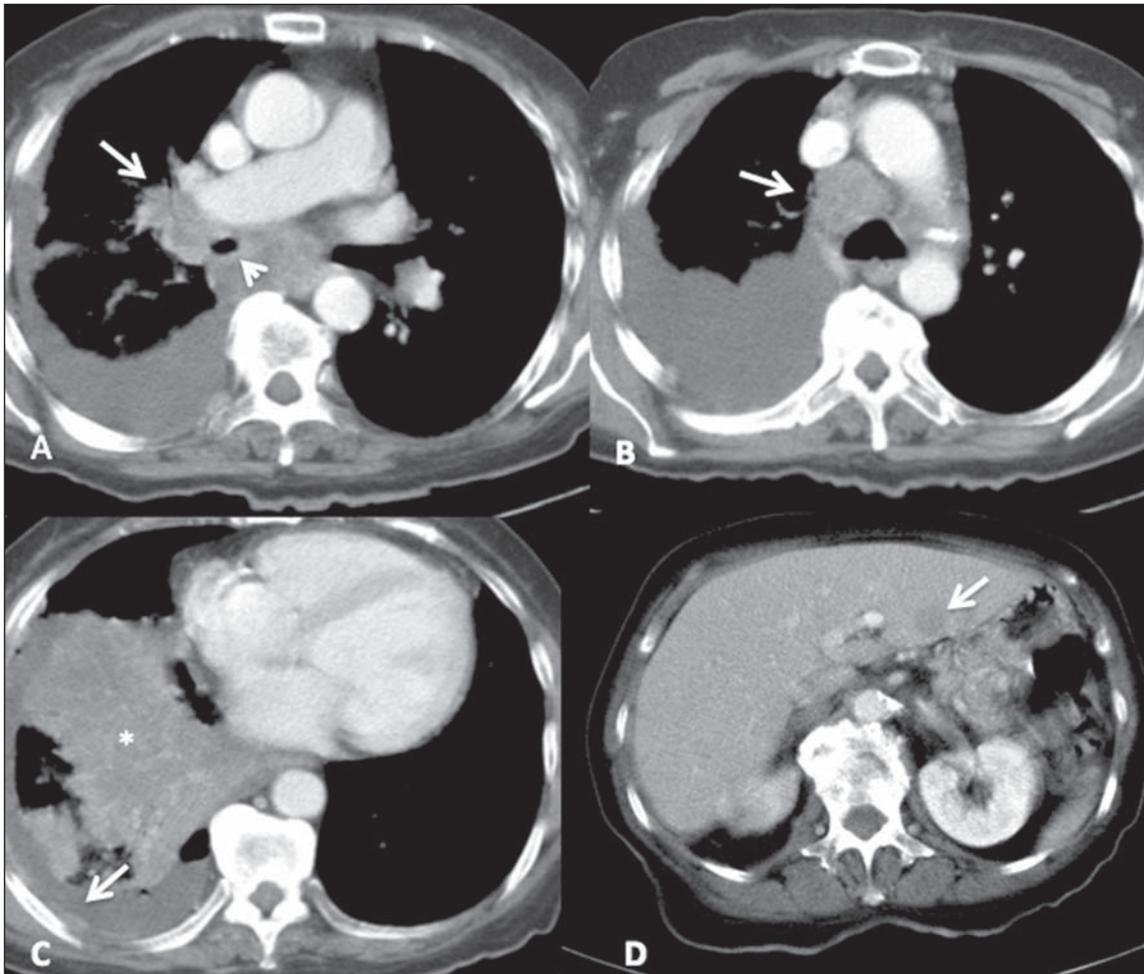
Figure 6. Small-cell lung cancer. Characteristic lesion identified on contrast-enhanced chest CT with mediastinal window. Right, heterogeneous central mass with ill-defined margins, causing narrowing (arrow head on **A**) with invasion of the right pulmonary artery (arrow on **A**). One observes prominent mediastinal lymphadenopathy (arrow on **B**), signs of pleural cacinomatosis at right, with effusion and areas of thickening which enhance after contrast injection (arrow on **C**), also associated with parenchymal consolidation in the right lower lobe due to probable pneumonia/atelectasis (asterisk on **C**). On the images of the upper abdomen, it was possible to identify a hypodense nodular lesion in the left hepatic lobe (arrow on **D**), compatible with metastasis.

DISCUSSION

Neuroendocrine tumors of the lung originate in the bronchial mucosa and present similar histopathological characteristics, but present a wide clinical spectrum with behavior ranging from the relatively indolent and well differentiated typical carcinoid lesion to the most aggressive lung tumor, the SCLC[6]. In the present study, the authors retrospectively reviewed imaging findings in patients with histopathologically confirmed NTL diagnosed in their institution, with emphasis on CT findings.

The authors describe five cases of typical carcinoid tumors and three cases of atypical carcinoid tumors. Carcinoid tumors occur most frequently in the gastrointestinal tract (80% to 90%), with bron-

chial or lung carcinoid tumors being represented by the typical carcinoid type in most cases (approximately 90%) and less frequently by the atypical carcinoid type[7]. Atypical carcinoid tumors are assciated with smoking, most commonly affecting male patients (2:1) and at older ages (59 years, on average), while typical carcinoid tumors lack established association with smoking, affecting younger patients of both genders. Typical carcinoid tumors represent the most common lung neoplasia in the childhood and most frequently are diagnosed at less advanced clinical stages, rarely with metastases and progressing with longer survival as compared with atypical carcinoid tumors[8]. Among the presented cases, only one case (20%) of typical carcinoid tumor presented recurrence after

surgical resection of the primary lesion, while two patients (67%) with atypical tumors presented metastatic dissemination of the disease, and one (33%) progressed to death.

In the present study, the authors found only one case of central endobronchial nodule characteristic of typical carcinoid tumor, but atypical carcinoid tumors were found as larger and more heterogeneous peripheral masses, more frequently with metastases at diagnosis or follow-up, likewise described in the literature. Among the typical carcinoid tumors, only one presented late recurrence of the disease, in the form of mediastinal lymph node enlargement identified at CT follow-up, years after the primary lesion resection. According to the medical literature, imaging findings

of both typical and atypical carcinoid tumors are similarly described, being mainly found as well-defined nodules or masses, sometimes lobulated, and when elongated, with the longer axis parallel to the bronchi. Most commonly, the lesions are central, next to the source bronchi and present punctiform or diffuse calcifications identified at CT in up to 30% of the cases. Carcinoid tumors tend to be well vascularized, with prominent contrast enhancement, which also aids in the differentiation between lesions and the commonly associated distal secondary changes (pneumonia, atectasis and bronchi with mucoid impaction)[9]. Despite their similar characteristics, one describes that the presence of a central, well-defined nodule causing narrowing, deformity or obstruction of a bronchus, especially if containing calcifications, is suggestive of a typical carcinoid tumor. On the other hand, atypical carcinoid tumors tend to be larger, more peripheral (distal to the segmental bronchus) and more heterogeneous, besides presenting a higher incidence of metastatic lesions at the diagnostic imaging[10].

In the present study, the authors described three cases of LCNC, all of them presenting as peripheral heterogeneous masses associated with metatastic disease, and none of the lesions with calcifications. LCNC was the fourth and last tumor subtype to be recognized as a neuroendocrine tumor of the lung, with characteristics that make it different from the typical and atypical carcinoid tumors as well as from the SCLC[3]. It is predominantly found in men (2.5 times greater incidence than in women), above the age of 60, and in 60% of the cases in association with smoking. The prognosis for patients with LCNC is poorer than for patients with the other NSCLC types, with lower five-year survival rate[11]. However, the imaging findings are described as being similar to those of most adenocarcinomas and squamous cell carcinomas, with predominance of nodules or peripheral masses, irregular or spiculated margins, heterogeneous density with foci of necrosis and less frequently with calcifications (approximately 9%). Pleural thickening or effusion are also commonly described[12]. Interestingly, in the present review, one patient was a 36-year-old woman.

Two (67%) patients with LCNC progressed to death months after the diagnosis, despite of the treatment.

In the present study, the authors described 11 cases of patients with SCLC. Lesions were similar to those described as most characteristic in the medical literature, with no isolated findings of nodule or peripheral mass. All SCLC patients aready presented extensive disease at the moment of diagnosis and 10 (90%) patients progressed to death few months after diagnosis. Small-cell lung cancer represents approximately 20% of all bronchogenic carcinomas, is the lung neoplasia with stronger association with smoking and affects individuas at mean age of 70 years[6]. The literature reports that, at the moment of diagnosis, the patient usually presents advanced disease with metastasis, mainly to bones, liver, adrenal glands or brain[13]. The SCLC lesions are central in most cases and present in association with hilar and/or mediastinal lymph node enlargement, with a confluent aspect, many times forming large, infiltrating masses, and leading to the displacement or narrowing of the tracheobronchial tree and central vessels. Findings of atectasis, other lung lesions and pleural effusion are common. Calcifications are described as being present in up to 23% of cases. In the present study, lesions with calcifications were not found. More rarely, SCLC presents as a peripheral lung lesion without lymph node enlargement, and in such cases it may be confused with other types of bronchogenic carcinomas and with the other NTLs[1,14]. Probably, the present study's sample of SCLC was underestimated, considering its prevalence and the characteristic of specialized reference hospital of the authors' institution. The authors believe that such limitation of the present study was related to the fact that only cases with histopathological and immunohistochemical confirmation and radiological exams performed in their own institution were included.

In this series of cases, only one patient with lung neoplasia underwent MRI, with a typical carcinoid lesion presenting as a lung nodule. The role of MRI in the evaluation of lung neoplasms is increasing, particularly in the staging of lesions and in the clinical follow-up of the treatment. However, little has been reported in the literature[15] about MRI in the evaluation of NTL, and its role, particularly regarding diagnostic accuracy in the different histological types of NTL, still requires further investigation.

REFERENCES

1. Rosado-de-Christenson ML, Templeton PA, Moran CA. Bronchogenic carcinoma: radiologic pathologic correlation. Radiographics. 1994;14: 429–46.

2. Melmon KL, Sjoerdsma A, Mason DT. Distinctive clinical and therapeutic aspects of the syndrome associated with bronchial carcinoid tumors. Am J Med. 1965;39:568–81.

3. Travis WD, Linnoila RI, Tsokos MG, et al. Neuroendocrine tumors of the lung with proposed criteria for large-cell neuroendocrine carcinoma. An ultrastructural, immunohistochemical, and flow cytometric study of 35 cases. Am J Surg Pathol. 1991;15:529–53.

4. Travis WD, Colby TV, Corrin B, et al. Histological typing of lung and pleural tumors. 3rd ed. Berlin, Germany: Springer-Verlag; 1999.

5. Magid D, Siegelman SS, Eggleston JC, et al. Pulmonary carcinoid tumors: CT assessment. J Comput Assist Tomogr. 1989;13:244–7.

6. Chong S, Lee KS, Chung MJ, et al. Neuroendocrine tumors of the lung: clinical, pathologic, and imaging findings. Radiographics. 2006;26:41–57.

7. Modlin IM, Lye KD, Kidd M. A 5-decade analysis of 13,715 carcinoid tumors. Cancer. 2003;97: 934–59.

8. Ducrocq X, Thomas P, Massard G, et al. Operative risk and prognostic factors of typical bronchial carcinoid tumors. Ann Thorac Surg. 1998; 65:1410–4.

9. Zwiebel BR, Austin JH, Grimes MM. Bronchial carcinoid tumors: assessment with CT of location and intratumoral calcification in 31 patients. Radiology. 1991;179:483–6.

10. Jeung MY, Gasser B, Gangi A, et al. Bronchial carcinoid tumors of the thorax: spectrum of radiologic findings. Radiographics. 2002;22:351–65.

11. Paci M, Cavazza A, Annessi V, et al. Large cell neuroendocrine carcinoma of the lung: a 10-year clinicopathologic retrospective study. Ann Thorac Surg. 2004;77:1163–7.

12. Oshiro Y, Kusumoto M, Matsuno Y, et al. CT findings of surgically resected large cell neuroendocrine carcinoma of the lung in 38 patients. AJR Am J Roentgenol. 2004;182:87–91.

13. Micke P, Faldum A, Metz T, et al. Staging small cell lung cancer: Veterans Administration Lung Study Group versus International Association for the Study of Lung Cancer – what limits limited disease? Lung Cancer. 2002;37:271–6.

14. Pearlberg JL, Sandler MA, Lewis JW Jr, et al. Small-cell bronchogenic carcinoma: CT evaluation. AJR Am J Roentgenol. 1988;150:265–8.

15. Douek PC, Simoni L, Revel D, et al. Diagnosis of bronchial carcinoid tumor by ultrafast contrast-enhanced MR imaging. AJR Am J Roentgenol. 1994;163:563–4.